

Объединенный
институт
ядерных
исследований
Дубна

799/2-80

25/2-80
E4 - 12815

A.G.Baryshnikov, V.B.Belyaev, L.D.Blokhintsev,
B.F.Irgaziev, Yu.V.Orlov

SCATTERING AND REACTIONS
IN THE FOUR-NUCLEON SYSTEM WITHIN
THE K-MATRIX FORMALISM

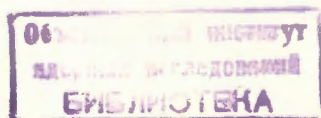
1979

E4 - 12815

**A.G.Baryshnikov, V.B.Belyaev, L.D.Blokhintsev,
B.F.Irgaziev, Yu.V.Orlov**

**SCATTERING AND REACTIONS
IN THE FOUR-NUCLEON SYSTEM WITHIN
THE K-MATRIX FORMALISM**

Submitted to ЯФ



Барышников А.Г. и др.

E4 - 12815

Рассеяние и реакции в системе 4 нуклонов
в рамках K-матричного формализма

Формализм многоканальной K-матрицы используется для изучения бинарных процессов в 4-нуклонных системах. Элементы K-матрицы аппроксимируются диаграммами Фейнмана, соответствующими механизму обмена одним и двумя нуклонами.

Работа выполнена в Лаборатории теоретической физики ОИЯИ.

Препринт Объединенного института ядерных исследований. Дубна 1979

Baryshnikov A.G. et al.

E4 - 12815

Scattering and Reactions in the Four-Nucleon
System within the K-Matrix Formalism

The multi-channel K-matrix formalism is used to study the binary processes in four-nucleon systems. The K-matrix elements are approximated by Feynman diagrams corresponding to the exchange by one and two-nucleon.

The investigation has been performed at the Laboratory of Theoretical Physics, JINR.

Preprint of the Joint Institute for Nuclear Research. Dubna 1979

1. INTRODUCTION

At present the description of three-nucleon systems within the Faddeev equations is not a complicated task, except for the problem of continuous spectrum with realistic NN-interaction. At the same time, the solution of the four-body integral Faddeev-Yakubovsky equations ^{1/} even with the simplest potentials encounters great difficulties, and there are only a few relevant papers. The binding energies of the ground and first excited state of ⁴He for the separable Yamaguchi NN-potential were found from the Faddeev-Yakubovsky equations by the Bateman method ^{2/} and by the Gilbert-Schmidt method ^{3/}. The latter was also applied for the description of discrete ⁴He states for the case of the Malfliet - Tjon potential ^{4/}. The nuclear vertex constants (coupling constants) ^{5/} for the vertices $\alpha \rightarrow {}^3\text{H}({}^3\text{He}) + p(n)$ and $\alpha \rightarrow d+d$ were calculated in paper ^{6/} by solving the Faddeev-Yakubovsky equations for the Yamaguchi potential.

As for the continuous spectrum of the four-nucleon system, paper ^{7/} appears to be the only paper in which the Faddeev-Yakubovsky equations (for the Malfliet - Tjon potential) are used below the $d+d$ threshold. Besides, $n^3\text{He}$ - and $n^3\text{H}$ -scattering lengths were calculated by solving the Faddeev-Yakubovsky equations for the Yamaguchi potential in paper ^{8/}.

A direct solution of these equations above the $d+d$ threshold is a very complicated problem which has not been solved yet. On the other hand, the four-nucleon system may provide more complete information about NN-interaction and about the efficiency of different theoretical approaches as compared to the three-nucleon system. The attempts were made to describe approximately the scattering and reactions

in the four-nucleon system within the framework of the K-matrix formalism^{9,12/}. In particular, in paper^{/11/} the free terms of the Faddeev-Yakubovsky equations calculated for the Yamaguchi potential were used as the K-matrix elements for different binary processes in the four-nucleon system.

In this paper we have used the multichannel K-matrix formalism to study the two-particle processes in the four-nucleon system, K-matrix elements being approximated by the amplitudes of the Feynman diagrams corresponding to the one- and two-nucleon exchange mechanisms. To calculate these amplitudes we have used the wave functions of nuclei ³H (or ³He) obtained earlier^{/13,14/} by solving the Faddeev equations for three different NN-potentials. The calculated differential cross sections are in satisfactory agreement with the experimental data. We have also analyzed the dependence of the results on the form of NN-potential and the role of channel coupling and the singlet NN-pair exchange mechanism. We have not used any free parameters in our calculations.

2. K-MATRIX FORMALISM

In this paper we use the same normalization of matrix elements of K-, S- and T-matrices as in the papers^{/11,15/}. In what follows we take into account only the two-particle channels in the four-nucleon system. We use the central potentials and do not take into account the Coulomb interaction and other effects violating the isotopic invariance. We consider only the s-states of nuclei ²H, ³H, and ³He. In such an approach the conserved quantities are the channel spin S, the total isospin of the four-nucleon system T, and the channel orbital momentum ℓ . The Heitler equations connecting the partial matrix elements of the T-matrix ($T_{ik}^{ST\ell}$) and K-matrix ($K_{ik}^{ST\ell}$) for the transition $i \rightarrow k$ have the form

$$T_{ik}^{ST\ell}(E_k) = K_{ik}^{ST\ell}(E_k) - i \sum_{j=1}^n \rho_j K_{ij}^{ST\ell}(E_j) T_{jk}^{ST\ell}(E_k), \quad (1)$$

where $\rho_j = \mu_j p_j / 2\pi$, μ_j and p_j are the reduced mass and relative momentum in the channel j , $E_j = p_j^2 / 2\mu_j$, n is a number of opened channels.

The differential cross section of the reaction $A_k + X_k \rightarrow A_k + X_k$ for unpolarized particles is

$$\frac{d\sigma_{ik}}{d\Omega} = \frac{\mu_i \mu_k}{4\pi^2} \frac{p_k}{p_i} \frac{1}{(2J_{A_i}+1)(2J_{X_i}+1)STT'} \sum (2S+1)(T_{A_i} r_{A_i} T_{X_i} r_{X_i} |T_r) \times$$

$$\times (T_{A_i} r_{A_i} T_{X_i} r_{X_i} |T_r')(T_{A_k} r_{A_k} T_{X_k} r_{X_k} |T_r)(T_{A_k} r_{A_k} T_{X_k} r_{X_k} |T_r') \times$$

$$\times T_{ik}^{ST}(E_k, Z_{ik}) [T_{ik}^{ST'}(E_k, Z_{ik})]^*,$$

$$T_{ik}^{ST}(E_k, Z_{ik}) = \sum_{\ell=0}^{\infty} (2\ell+1) T_{ik}^{ST\ell}(E_k) P_{\ell}(Z_{ik}),$$

where $P(Z)$ are the Legendre polynomials, $Z_{ik} = \cos \theta_{ik}$, θ_{ik} is the scattering angle in the CM-system, J_a , T_a and r_a are the spin, isospin and isospin projection of a nucleus a and $r = r_{A_i} + r_{X_i} = r_{A_k} + r_{X_k}$. Note, that the K-matrix is symmetric $K_{ij}^{ST\ell} = K_{ji}^{ST\ell}$.

Equation (1) is a system of linear algebraic equations. Omitting the indices S, T and ℓ for simplicity, we write down their solutions at $n=1$ and $n=2$.

$$T_{11} = K_{11} / (1 + i\rho_1 K_{11}), \quad (n=1), \quad (3)$$

$$T_{11} = [(1 + i\rho_2 K_{22})K_{11} - i\rho_2 K_{12}^2] / D,$$

$$T_{22} = [(1 + i\rho_1 K_{11})K_{22} - i\rho_1 K_{12}^2] / D, \quad (4)$$

$$T_{12} = K_{12} / D, \quad D = (1 + i\rho_1 K_{11})(1 + i\rho_2 K_{22}) + \rho_1 \rho_2 K_{12}^2, \quad (n=2).$$

3. THE CHOICE OF K-MATRIX ELEMENTS

In the four-nucleon system there are two-particle channels: $N+T$ (channel 1) and $d+d$ (channel 2), where $N=n,p$ and $T = ^3H, ^3He$. We proceed from the assumption^{/14/} that the main contribution to the K-matrix elements which are considered as analytic functions of Z_{ik} is given by the nearest to the physical region singularities of these functions corresponding to the simplest Feynman diagrams. As is shown in^{/15/} the position of the nearest singularities in Z_{ik} and their power (i.e., residues at poles or discontinuities on cuts) for K- and T-matrices coincide.

In accordance with the aforesaid we choose as K-matrix elements $K_{11}|N+T \rightarrow N+T|$ and $K_{12}|N+T \rightarrow d+d|$ the amplitudes of diagrams of Figs. 1 and 2, respectively, which co

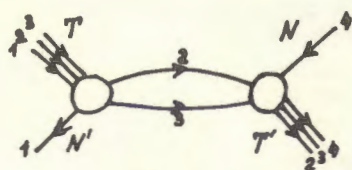


Fig. 1

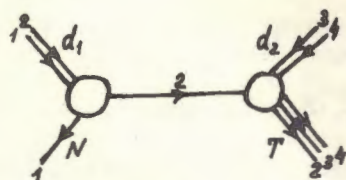


Fig. 2

correspond to the two- and one-nucleon transfer. As in paper ^{11/} we put $K_{22}=0$; this is somewhat justified by the absence of Born terms for the process $d+d \rightarrow d+d$ in the Faddeev-Yakubovsky equations.

Let us consider the amplitudes of diagrams in Figs. 1 and 2 in more detail. We proceed with the diagram of the two-nucleon exchange (Fig. 1). We shall consider a transfer of the correlated (interacting) nucleon pair. In this case the diagram of Fig. 1 can be written as Fig. 3 where f_{23} is

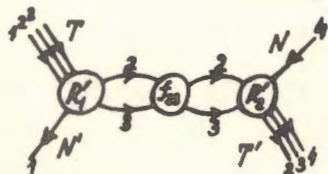


Fig. 3

the scattering amplitude of nucleons 2 and 3, $R'_1 = R_1^{(12)} + R_1^{(13)} = R_1 - R_1^{(23)}$ is the vertex function for the decay $(123) \rightarrow 1 + 2 + 3$ with the subtracted terms which correspond to the Faddeev component ending with the interaction of nucleons 2 and 3, and analogously $R'_2 = R_2^{(24)} + R_2^{(34)} = R_2 - R_2^{(23)}$ is the "truncated" vertex of synthesis $2 + 3 + 4 \rightarrow (234)$ which contains no terms beginning with the interaction of 2 with 3.

Note, that in the case of diagrams of Figs. 1 and 3, it does not matter whether they are the four-dimensional non-relativistic diagrams or three-dimensional "Schrödinger"

diagrams, since the analytic properties of the vertex functions $R_{1,2}^{(i,j)}$ and f_{ij} are such (see ^{16/}) that the four-dimensional form is reduced to the three-dimensional one by integrating over the energies of virtual particles. This integration is performed by calculating the residue at pole corresponding to one of the virtual lines 2 or 3*. In the three-dimensional representation the vertex functions $R^{(ij)}$ are proportional to the corresponding Faddeev components ψ^{ij} of the three-particle wave functions. Including the scattering amplitude f_{23} in Fig. 3 and virtual lines 2 and 3 entering into it from left (right) in the left (right) vertex and using the Faddeev equations, we obtain the diagram in Fig. 1. The left (right) vertex of this diagram corresponds to the quantity $R_1^{(23)} (R_2^{(23)})$, whereas the right (left) vertex corresponds to $R_2^{(24)} + R_2^{(34)} (R_1^{(12)} + R_1^{(13)})$. Finally the amplitude of the diagram in Fig. 1 can be written as

$$M_1 = \frac{6}{(2\pi)^3} \int \psi^{23}(\vec{q}_{23}, \vec{Q}_{1,23}) \left[\epsilon_T + \frac{\vec{q}_{23}^2}{m_N} + \frac{\vec{Q}_{1,23}^2}{4/3 m_N} \right] \times \quad (5)$$

$$\times [\psi^{24}(\vec{q}_{24}, \vec{Q}_{3,24}) + \psi^{34}(\vec{q}_{34}, \vec{Q}_{2,34})] d\vec{q}_{23}.$$

Here $\psi^{ij}(\vec{q}, \vec{Q})$ are the Faddeev components of the wave functions of the three-particle bound states, $\vec{q}_{ij} = \frac{1}{2}(\vec{k}_i - \vec{k}_j)$, $\vec{Q}_{i,jk} = \frac{1}{3}[2\vec{k}_i - (\vec{k}_j + \vec{k}_k)]$ are the Jacobi momenta, \vec{k}_i is the momentum of nucleon i , $\epsilon_T > 0$ is the binding energy of ${}^3\text{H}$ (or ${}^3\text{He}$), and m_N is the nucleon mass, factor 6 is due to the identity of nucleons. The wave function $\psi = \sum \psi^{ij}$ is normalized by the condition $(2\pi)^{-6} \int |\psi(\vec{q}, \vec{Q})|^2 d\vec{q} d\vec{Q} = 1$.

In Eq. (5) the spin and isospin variables are not written explicitly. Introducing the spin (χ) and isospin (ξ) wave functions, one can write ψ^{ij} in the usual form

$$\psi^{ij} = v_{ij} \chi_{ij}'' \xi'_{ij} - u_{ij} \chi_{ij}' \xi''_{ij}, \quad (6)$$

where the functions of momentum variables v_{ij} and u_{ij} correspond to the triplet and singlet spin states of a pair of

*Note, that for arbitrary diagrams in the four-nucleon system such a simple connection between three- and four-dimensional formalism does not hold.

nucleons i and j (we take into account the even states of a nucleon pair only).

Taking the amplitude (5) as the matrix element K_{11} for the process $N+T \rightarrow N+T$, we finally have

$$K_{11}^{ST\ell} = \frac{1}{2} \int_{-1}^1 K_{11}^{ST}(Z) P_{\ell}(Z) dZ, \quad (7)$$

$$K_{11}^{ST}(Z) = M_1 = 12 \sum_{(j^i)=(01),(10)} W(\frac{1}{2} \frac{1}{2} \frac{1}{2}; jS) W(\frac{1}{2} \frac{1}{2} \frac{1}{2}; iT) R^{(j)}(Z),$$

where

$$R^{(1)} = \frac{1}{2(2\pi)^3} \int d\vec{q}_{23} v(\vec{q}_{23}, \vec{Q}_{1,23}) L(\vec{q}_{23}, \vec{Q}_{1,23}) [v(\vec{q}_{31}, \vec{Q}_{2,31}) + 3u(\vec{q}_{31}, \vec{Q}_{2,31})], \quad (8)$$

$$R^{(0)} = \frac{1}{2(2\pi)^3} \int dq_{23} u(q_{23}, Q_{1,23}) L(q_{23}, Q_{1,23}) [u(q_{31}, Q_{2,31}) + 3v(q_{31}, Q_{2,31})],$$

$$L(\vec{q}, \vec{Q}) = \epsilon_T + \frac{q^2}{m_N} + \frac{Q^2}{(4/3)m_N},$$

$Z = \vec{p}\vec{p}'/pp'$, and \vec{p} and \vec{p}' are the momenta of incident and scattered nucleons in the c.m.s. system. The terms with $j=1$ and $j=0$ in (7) correspond to the transfer of a nucleon pair in the triplet and singlet spin states.

Expressions (7) and (8) correspond to the transfer of the correlated nucleon pair and comprise, in particular, the deuteron transfer. Various mechanisms of the transfer of a noncorrelated pair, which do not enter into the K -matrix, are partially taken into account in T -matrix due to the channel coupling expressed by equations (1) and (4).

By taking into account the identity of deuterons the amplitude of the diagram in Fig. 2, which is used as the K -matrix element K_{12} , can be written in the form

$$K_{12}^{ST\ell} = \frac{1}{2} \int_{-1}^1 K_{12}^{ST}(Z) P_{\ell}(Z) dZ,$$

$$K_{12}^{ST}(Z) = -\frac{2\sqrt{3}m_N}{pp'} W(\frac{1}{2} \frac{1}{2} 1; 1S) \left[\frac{w_{TdN}(Q) w_d(Q)}{\zeta - Z} + (-1) \frac{w_{TdN}(\tilde{Q}) w_d(\tilde{Q})}{\zeta + Z} \right], \quad (9)$$

where $\vec{p}(\vec{p}')$ is the relative momentum in the initial (final) state, w_{TdN} is the vertex function for the decay $T \rightarrow d + N$, w_d is the vertex function for the process $d \rightarrow p + n$, $Q^2 = \frac{4}{9} p^2 + p'^2 - \frac{4}{3} pp'Z$, $q^2 = p^2 + \frac{1}{4} p'^2 - pp'Z$, \tilde{Q}^2 , and \tilde{q}^2 differ from Q^2 and q^2 by the substitution $Z \rightarrow -Z$, $\epsilon_d > 0$ is the deuteron binding energy, $Z = \vec{p}\vec{p}'/pp'$, and ζ is the position of the pole singularity for the diagram in fig. 2

$$\zeta = \frac{1}{3} \frac{p}{p'} + \frac{3}{4} \frac{p'}{p} + \frac{m_N(\epsilon_T - \epsilon_d)}{pp'}. \quad (10)$$

The vertex functions w_{TdN} and w_d are defined by the formulae

$$w_{TdN}(Q) = -\left(\frac{3}{4} \frac{Q^2}{m_N} + \epsilon_T - \epsilon_d\right) \int \frac{d\vec{q}}{(2\pi)^3} \left\{ v(q, Q) + \frac{1}{2} v\left(\left|\frac{\vec{q}}{2} + \frac{3\vec{Q}}{4}\right|, \left|\vec{q} - \frac{\vec{Q}}{2}\right|\right) + \frac{3}{2} u\left(\left|\frac{\vec{q}}{2} + \frac{3\vec{Q}}{4}\right|, \left|\vec{q} - \frac{\vec{Q}}{2}\right|\right) \right\} \phi_d(q), \quad (11)$$

$$w_d(Q) = -\left(\frac{Q^2}{m} + \epsilon_d\right) \phi_d(Q), \quad (12)$$

where $\phi_d(Q)$ is the deuteron wave function ($\int |\phi_d(Q)|^2 d\vec{q} / (2\pi)^3 = 1$).

In our calculation we have used the matrix elements M_1 and the vertex functions w_{TdN} and w_d obtained earlier in paper^{14/} by solving the Faddeev equations for three different local NN-potentials, the Malfliet-Tjon (MT), Darevich-Green (DG) and the modified Bressel-Kerman-Ruben (BKR) potentials.

4. DISCUSSION OF THE RESULTS OBTAINED FOR THE SPECIFIC PROCESSES

The differential cross sections for the elastic scattering and reactions in the four-nucleon system have been calculated for several values of energy for MT, DG and BKR-potentials. The role of the channel coupling and of the singlet NN-pair exchange mechanism has been analyzed for different variants of calculation. Besides the calculations taking into account both the channels $N+T$ and $d+d$, the variant 1, to calculate the differential cross sections of

the elastic $p^3\text{He}$ and $p^3\text{H}$ scattering and reaction (p, n) we have used the one-channel approximation, the variant 2. To evaluate the contribution of the singlet pair exchange mechanism within the above two variants, we have neglected the singlet state of the transferred nucleon pair in the K-matrix element for the process $N+T \rightarrow N+T$ (variants 3 and 4). In this case, in formula (7) instead of the sum in $j=0,1$ there is only one term with $j=1$ corresponding to the NN-pair exchange in the triplet state. In all the calculations we have taken into account partial waves with $l \leq 8$.

$^3\text{He}(p, p)^3\text{He}$. In this case the states with $S=0,1$ and $T=1$ are possible, the channel $d+d$ is absent and the variants 1 and 3 coincide with the variants 2 and 4 (one-channel scattering), respectively.

For this process we have calculated the differential cross sections with three NN-potentials at the lab. proton energies $E_p = 9.75, 13.6, 16.23, 19.48, 30.6$ and 49.5 MeV in the angular range $60-180^\circ$ in the c.m.s.

We have chosen this range since the K-matrix elements we have used for elastic scattering $N+T \rightarrow N+T$ are singular in $\cos\theta$, when $\cos\theta < -1$ and cannot reproduce the experimental cross sections in the forward hemisphere. We also have disregarded the Coulomb interaction which is essential at small angles. The scattering differential cross sections calculated in the K-matrix approach are plotted in Fig. 4 for the incident proton energy $9.75, 19.48, 30.6$ MeV for BKR, DG and MT potentials. As one can see from Fig. 4, the theoretical curves are in a qualitative agreement with experiment at angles $\theta_{\text{C.M.}} > 120^\circ$. As in the case of the Yamaguchi potential, the best agreement with experiment is achieved at $E = 30.6$ MeV. At all energies theoretical curves have a steeper rise for the backward angles and lay lower than experimental points at angles $\theta_{\text{C.M.}} \geq 150^\circ$. The theoretical differential cross sections calculated for different NN-potentials do not differ much from each other, this difference growing when the energy increases.

Figure 4 also shows the results of calculation in the T-matrix Born approximation for ("Born" curves)* the MT potential. At $E_p = 9.75$ MeV the Born curve is rather higher than

* In the Born approximation the amplitudes of diagrams, Figs. 1 and 2, are taken as T-matrix elements for corresponding processes.

the K-matrix curve and experimental points. As was to be expected, the difference between the K-matrix and Born curve decreases when the energy increases.

In this Figure the dashed curve represents the theoretical cross sections calculated in the K-matrix approach neglecting the singlet pair exchange in the K-matrix element, K_{11} (variant 4). For all energies, the differential cross sections calculated without that exchange are lower than those with it throughout the whole angular range considered. The neglect of the singlet pair exchange diminishes the calculated cross sections at $\theta_{\text{C.M.}} = 180^\circ$ by 20-25% throughout the whole energy interval for all three NN-potentials.

$^3\text{H}(p, p)^3\text{H}$. In this case $S=0,1$ and $T=0,1$ and both the channels, $p+^3\text{H}$ and $d+d$ are allowed. For the elastic scattering $^3\text{H}+p \rightarrow ^3\text{H}+p$ the nucleon pair can be transferred only in the singlet state therefore the neglect of the singlet pair exchange in variant 3 results in $K_{11}^{\text{ST}} = 0$, and the nonzero differential cross section in that case is completely due to the coupling to the $d+d$ channel. In Fig. 5 we have plotted the $^3\text{H}(p, p)^3\text{H}$ differential cross sections calculated in different variants at $E_p = 13.6$ MeV (a) and $E_p = 19.48$ MeV (b) for three NN potentials. The theoretical curves are in satisfactory agreement with experiment at $\theta_{\text{C.M.}} \geq 120^\circ$, and even in good agreement at 19.48 MeV. Note that for the Yamaguchi potential there was no quantitative agreement [11]. Curves 1 are the cross section in variant 1, i.e., calculated with taking into account both the channels, for the potentials MT (solid curve), DG (dashed curve), and BKR (dashed-dotted line). It is seen that the curves for different potentials do not differ much from each other. Curves 2 are the cross sections calculated in the one-channel approximation (without the $d+d$ channel), and curves 3 are calculated with the channel $d+d$ and without the singlet pair exchange in the matrix element $K_{11} (K_{11}^{\text{ST}} = 0)$. Curves 3 are rather higher than curves 2 and more close to the exact calculations (curves 1). This means that the $^3\text{H}(p, p)^3\text{H}$ scattering in our model is mainly due to the coupling to $d+d$ channel and depends weakly on the magnitude of the K-matrix element for the elastic NT-channel. Therefore, the neglect of the $d+d$ -channel decreases the differential cross section at 180° by a factor of two as compared to the exact calculation, and the neglect of K_{11} results in the 20% - decrease of the cross section only. In order to understand the reason for such

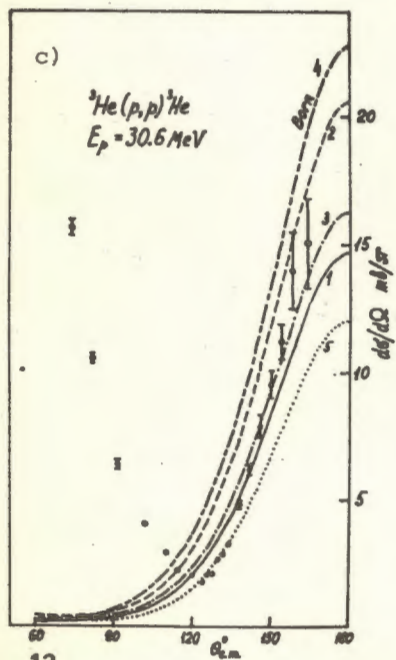
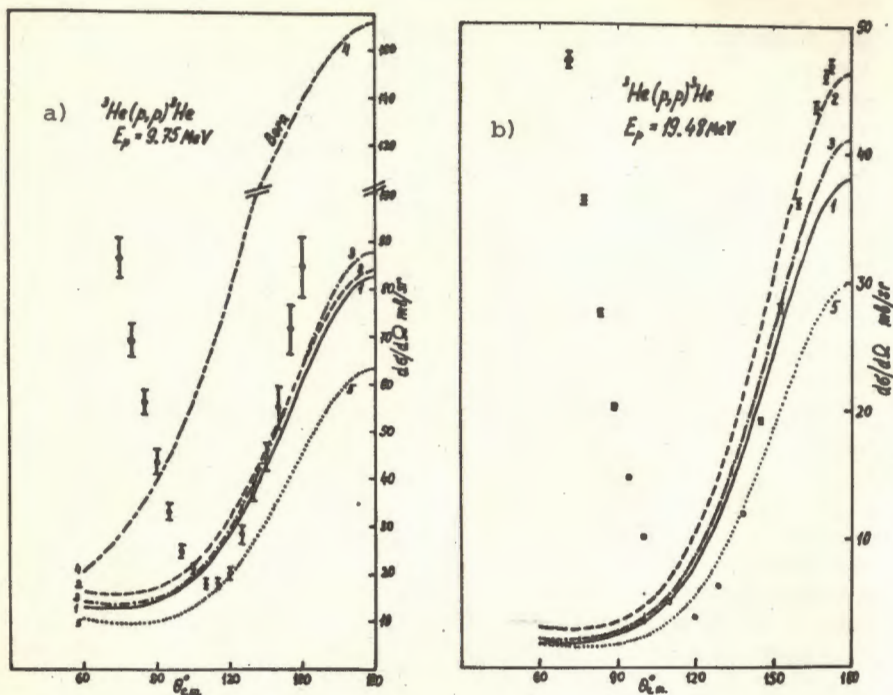


Fig. 4. Elastic $p^3\text{He}$ -scattering differential cross sections at the proton energies 9.75 MeV (a), 19.48 MeV (b), 30.6 MeV (c), calculated for different NN-potentials; the curve 1 is for the BKR potential; 2, for DG; and 3, for MT. The curve 4 is obtained in the Born approximation for the T-matrix. The curve 5 is obtained neglecting the singlet NN-pair exchange in the matrix element K_{11} for the BKR potential. The experimental points are taken from refs. ¹⁷(9.75 MeV), ¹⁸(19.48 MeV), and ¹⁹(30.6 MeV).

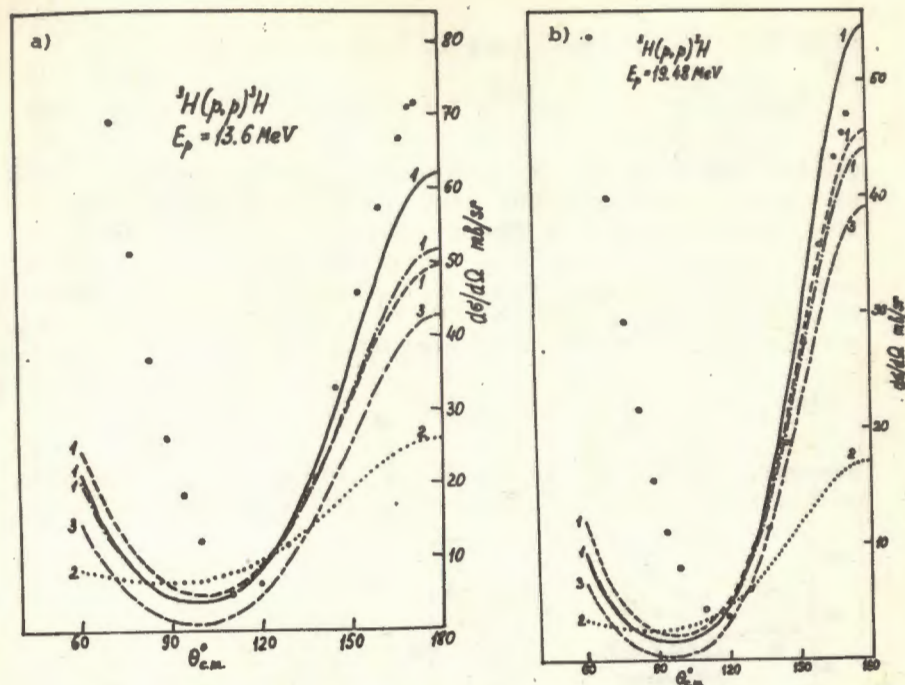


Fig. 5. The elastic $p^3\text{H}$ -scattering differential cross sections at the proton energies 13.6 MeV (a) and 19.48 MeV (b). The curves are calculated as explained in the text. The experimental data are taken from paper ²⁰.

a dependence, let us consider the formulae (4) which express the partial T-matrix elements in terms of K-matrix for two channels taken into consideration. In our case N+T is channel 1, and d+d is channel 2, $K_{22}=0$ and formulae (4) take the form

$$T_{11} = (K_{11} - i\rho_2 K_{12}^2) / D, \quad T_{22} = -i\rho_1 K_{12}^2 / D, \quad T_{12} = K_{12} / D, \quad (13)$$

$$D = 1 + i\rho_1 K_{11} + \rho_1 \rho_2 K_{12}^2.$$

Hence

$$\begin{aligned} \text{Re} T_{11} &= K_{11} / |D|^2, \quad \text{Im} T_{11} = -[\rho_1 K_{11}^2 + \rho_2 K_{12}^2 (1 + \rho_1 \rho_2 K_{12}^2)] / |D|^2, \\ |D|^2 &= \rho_1^2 K_{11}^2 + (1 + \rho_1 \rho_2 K_{12}^2)^2; \end{aligned} \quad (14)$$

From numerical calculations it follows that for $l = 0$

$$K_{11}/\rho_2 K_{12}^2 \ll 1, \quad \rho_1 \rho_2 K_{12}^2 \gg 1. \quad (15)$$

These conditions will be referred to as the strong coupling of channels (SCC). If the conditions of SCC are satisfied then the relation (14) gives $\text{Im}T_{11} \approx -\rho_1^{-1}$ and $|\text{Re}T_{11}/\text{Im}T_{11}| = |\rho_1 K_{11}/\rho_1 \rho_2 K_{12}^2| \ll 1$ and $\text{Im}T_{11}$ does not depend on K_{11} and K_{12} and $\text{Re}T_{11}$ practically gives no contribution. Our calculations show that at $S=T=0$, $l=2^{\pm}$ e.g., the SCC (15) are worse fulfilled and we have approximately

$$\text{Im}T_{11} \approx -(\rho_1 + 1/\rho_2 K_{12}^2)^{-1}, \quad |\text{Re}T_{11}/\text{Im}T_{11}| \approx 0.14.$$

However, for $l = 0$, as for $l = 0$, $\text{Im}T_{11}$ mainly depends on K_{12} rather than on K_{11} , while $\text{Re}T_{11}$ depends both on

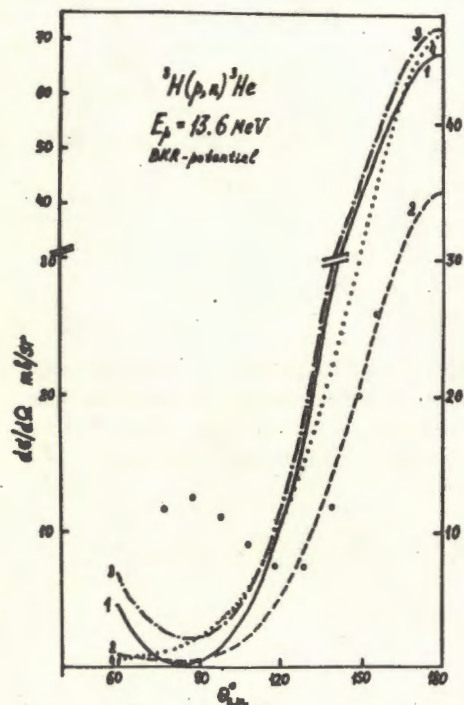


Fig. 6. Theoretical curves and experimental points^{20/} for the reaction ${}^3\text{H}(p, n){}^3\text{He}$ at the proton energy 13.6 MeV.

K_{12}^{STl} differs from zero only at $T=0$ and $S+l$ even.

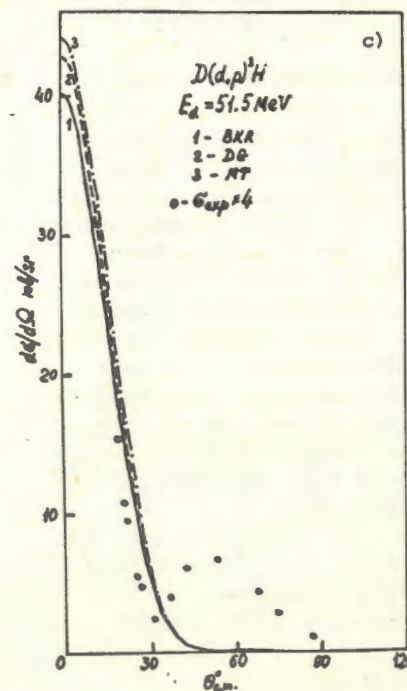
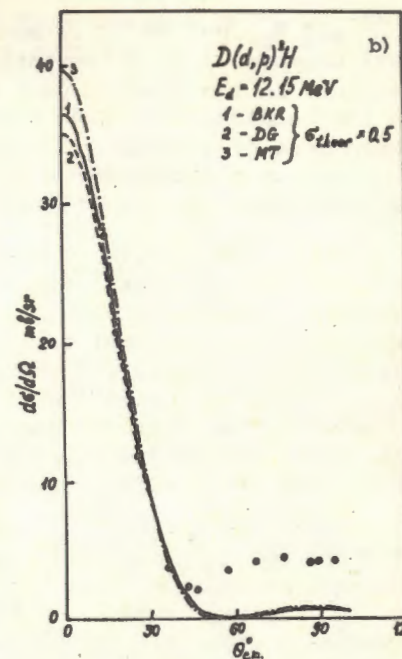
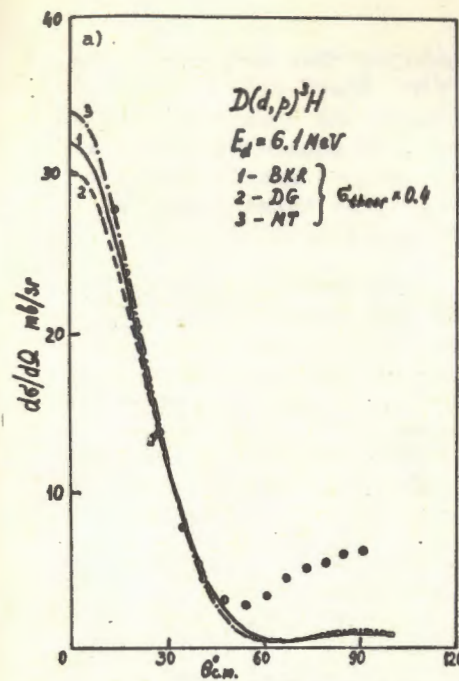


Fig. 7. The reaction $D(d,p){}^3\text{H}$ differential cross sections at the deuteron energies 6.1 MeV (a), 12.15 MeV (b) and 51.5 MeV (c). The curves are obtained as is explained in the text. The experimental points are taken from refs.^{21/} (12.15 MeV) and^{22/} (51.5 MeV).

K_{11} and K_{12} , but $\text{Re}T_{11}$ is much smaller than $\text{Im}T_{11}$. Thus, the weak dependence of differential $p^3\text{H}$ scattering cross sections on the singlet-pair exchange and strong dependence on the coupling to the $d+d$ channel is caused by the weak dependence of partial T_{11} -amplitudes on matrix elements K_{11} and strong dependence on K_{12} (that takes place, as is seen, when the conditions (15) are fulfilled).

$^3\text{H}(p, n)^3\text{He}$. Figure 6 shows the differential cross sections of reactions $^3\text{H}(p, n)^3\text{He}$ calculated in all four variants at proton energy 13.6 MeV for the BKR potential. With the $d+d$ channel taken into account the theoretical curves qualitatively reproduce the experimental rise at $\theta_{\text{C.M.}} \geq 120^\circ$ but exceed the experimental values by about a factor of two. All the conclusions concerning the singlet pair exchange mechanism and $d+d$ channel drawn for $p^3\text{H}$ scattering remain probably valid, as well.

$D(d, p)^3\text{H}$. Figure 7 shows the results of calculation of differential cross sections for reaction $D(d, p)^3\text{H}$ at deuteron energies 6.1 MeV (a), 12-15 MeV (b) and 51.5 MeV (c) for all the considered NN-potentials. The theoretical curves describe well the shape of experimental cross sections at small angles, but exceed them in absolute value (by a factor of 2-2.5 at 6.1 MeV and 4 at 51.5 MeV). In Fig. 7 there are shown the curves obtained in variant 1 and not shown those calculated in variant 3, i.e., without exchange of the singlet pair in the K-matrix element of $N+T \rightarrow N+T$. They almost coincide which means the weak dependence of the amplitude T_{12} on K_{11} . There also are not shown the results of calculation of the differential cross section of reaction $D(d, p)^3\text{H}$ in the T-matrix Born approximation. The corresponding Born curves are rather higher than the K-matrix curves and experimental points, especially at low energies. Thus, though in the case under consideration the coupling with other channels is weak (weak K_{11} -dependence), nevertheless, the Born approximation essentially differs from the K-matrix one. This testifies to the importance of the contribution of diagrams containing odd number of pole blocks K_{12} . As numerical calculation reveals the cross section for $D(d, p)^3\text{H}$ is less sensitive to the form of the NN-potential than the cross section for backward elastic $p^3\text{H}$ and $p^3\text{He}$ scattering. With growing energy this sensitivity increases for both processes, however, for the scattering this increase proceeds much faster.

Consider reaction $D(d, p)^3\text{H}$ from the view point of the two-channel problem with strong coupling in the K-matrix formalism. From formulae (14), under the conditions (15) it follows that:

$$\text{Re}T_{12} \approx \frac{1}{\rho_1 \rho_2 K_{12}}, \quad \text{Im}T_{12} \approx -\frac{1}{\rho_1 \rho_2 K_{12}} \cdot \frac{K_{11}}{\rho_2 K_{12}^2}, \quad (16)$$

$$|\text{Im}T_{12} / \text{Re}T_{12}| \approx \frac{K_{11}}{\rho_2 K_{12}^2} \ll 1.$$

Numerical calculations have shown that the conditions (15) are fulfilled for $\ell=0$ at low energies, as well. In particular, the K-matrix calculations of reaction $D(d, p)^3\text{H}$ at $E_d = 6.1$ MeV for the MT potential produce $|K_{11}/\rho_2 K_{12}^2| = 0.053 \ll 1$ and $\rho_1 \rho_2 K_{12}^2 = 54.2 \gg 1$ in the state $\ell=S=T=0$

while the approximate formulae (16) give the result for T_{12} within an accuracy of 2%. Formulae (16) provide an interesting result for the case of the SCC: $\text{Re}T_{12} \sim 1/K_{12}$, $\text{Im}T_{12} \sim K_{12}^{-3}$, i.e., the stronger the coupling of channels 1 and 2 (the larger K_{12} in the K-matrix approach), the smaller $|T_{12}|$. For the same state $S=T=0$ but for $\ell=2$ we have $|K_{11}/\rho_2 K_{12}^2| = 0.316$, $\rho_1 \rho_2 K_{12}^2 = 0.365$ and the conditions (15) SCC do not hold. With growing energy the conditions (15) are worse fulfilled.

$D(d, d)D$. In our approach $K_{22}=0$ therefore the agreement with experiment for elastic $d+d \rightarrow d+d$ scattering cannot be expected to be good. Indeed, the differential cross sections of elastic $D(d, d)D$ scattering calculated in the K-matrix formalism for several energy values are by a factor of 5-10 smaller than the experimental ones, and we do not cite them here.

CONCLUSION

It has been shown that the multi-channel K-matrix approach used in this paper allows us to obtain the correct shape of angular distributions at large scattering angles θ for processes $N+T \rightarrow N+T$ and at small θ (or $\pi-\theta$) for reaction $N+T \rightarrow d+d$. And for the $p^3\text{H}$ and $p^3\text{He}$ scattering the theory satisfactory reproduces also absolute values of cross sections.

Now we will discuss possibilities for improving an accuracy of the results obtained. First, one may include into consideration in K_{11} and K_{12} some other mechanisms, in particular, the transfer of the uncorrelated NN pair and triangular diagrams corresponding to the impulse approximation. Further, one should take into consideration the K-matrix element K_{22} for dd-scattering; here we put $K_{22} = 0$. As K_{22} , one may take the simplest diagrams drawn in Fig. 8. And finally, one may take into account the three- ($2N+d$) and four-particle ($4N$) channels though this complicates considerably a calculation procedure. We note that by including into the K-matrix triangular diagrams and those of Fig. 8b containing the NN-scattering amplitudes we partly take account of three- and four-particle states.

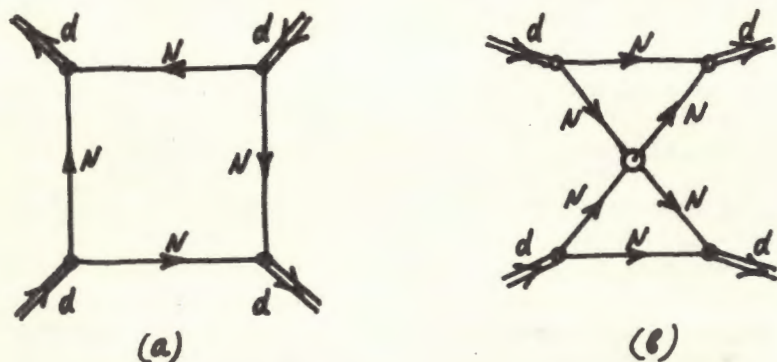


Fig. 8. The Feynman diagrams corresponding to the elastic dd-scattering.

REFERENCE

1. Yacubovsky O.A. *Yad.fiz.*, 1967, 5, p.1312;
Faddeev L.D. In: Proc. Problem Symp. on Nuclear Phys., Tbilisi, v. 1, Moscow, 1967, p. 43;
Faddeev L.D. In: Three Body Problem in Nuclear and Particle Physics, ed. by J.S.C.McKee and P.M.Rolph, North-Holland, Amsterdam, 1970, p.154.
2. Kharchenko V.F., Kuzmichev V.E. *Yad.fiz.*, 1973, 17, p. 1975; *ibid.* 1974, 20, p.334;
Kharchenko V.F., Kuzmichev V.E., Shadchin S.A. *Nucl. Phys.*, 1974, A226, p.71.

3. Narodetsky I.M., Halpern E.S., Lyakhovitsky V.M. *Pisma JETP*, 1973, 17, p.693; *Phys.Lett.*, 1973, 46B, p. 51; Narodetsky I.M. *Nucl.Phys.*, 1974, A221, p.191.
4. Tjon J.A. *Phys.Lett.*, 1975, 56B, p.217.
5. Blokhintsev L.D., Borbely I., Dolinsky E.I. In: *Particles and Nucleus*, 1977, 8, p.1189.
6. Baryshnikov A.G., Blokhintsev L.D., Narodetsky I.M. *Nucl. Phys.*, 1976, A272, p.327.
7. Tjon J.A. *Phys.Lett.*, 1976, 63B, p.391.
8. Kharchenko V.F., Levashev V.P. *Phys.Lett.*, 1976, 60B, p. 317.
9. Alt E.C., Grassberger P., Sandhas W. *Phys.Rev.*, 1970, C1, p.85.
10. Sawicki M., Namyslowski J.M. *Phys.Lett.*, 1976, 60B, p.331.
11. Baryshnikov A.G., Blokhintsev L.D., Narodetsky I.M. *Yad.fiz.*, 1977, 25, p.1167.
12. Perne R., Sandhas W. *Phys.Rev.Lett.*, 1977, 39, p.788.
13. Achmadhodjaev B., Belyaev V.B., Wrzcionco E. *Yad.fiz.*, 1970, 11, 1016;
14. Belyaev V.B., Wrzcionco E., Zubarev A.L. *Yad.fiz.*, 1970, 12, p.923; Belyaev V.B., Schulz M. *JINR,E4-6353*, Dubna, 1972.
14. Belyaev V.B., Irgasiev B.F., Orlov Yu.V. *JINR*, P4-8158, Dubna, 1974; *Yad.fiz.* 1976, 24, p.44.
15. Baryshnikov A.G., Blokhintsev L.D., Safronov A.N., Turovtsev V.V. *Nucl.Phys.*, 1974, A224, p.61.
16. Blokhintsev L.D., Dolinsky E.I. *Yad.fiz.*, 1967, 5, p.797.
17. Lovberg R.H. *Phys.Rev.*, 1956, 103, p.1393.
18. Hutson R.L. et al. *Phys.Rev.*, 1971, C4, p.17.
19. Langevin-Joliot H. et al. *Nucl.Phys.*, 1970, A158, p.309.
20. Detch J.L. et al. *Phys.Rev.*, 1971, C4, p.52.
21. Brolley J.E. et al. *Phys.Rev.*, 1957, 107, p.820.
22. Bruckmann H. et al. *Z.Phys.*, 1970, 230, p.383.

Received by Publishing Department
on September 28 1979.